Presented at the 37th European PV Solar Energy Conference and Exhibition, 7-11 September 2020

"GFVIS": A NON-DESTRUCTIVE METHOD FOR PHASE FRONT ANALYSIS BASED ON PHOTOS OF BRICK SIDES

T. Trötschler (nee Strauch)[1], A. S. Kovvali[1], S. Haddouk[1], A. Hess[1], P. Krenckel[1], H. Franz[2], C. Morche[2], S. Riepe[1], M. Demant[1], S. Rein[1]
[1]Fraunhofer Institute for Solar Energy Systems ISE, Heidenhofstr. 2, 79110 Freiburg i. Br., Germany
[2] ALD Vacuum Technologies GmbH, Wilhelm-Rohn-Str. 35, 63450 Hanau, Germany
Phone: +49 761 - 4588 5651; e-mail: matthias.demant@ise.fraunhofer.de

ABSTRACT: Blocking parasitic grain ingrowth in the ingot parts of cast-mono Si material close to crucible walls increases the outcome of purely monocrystalline wafers. This is one of the prerequisites for cast-mono to compete with Czochralski mono-crystalline Silicon as a less costly material with comparative quality. Phase boundary engineering plays a crucial role in the optimization of the crystallization process in terms of grain ingrowth from the edges but also for reducing stress and therefore dislocation generation and multiplication. Established methods for phase front measurements are destructive and/or time-consuming. We present a non-destructive method for phase front analysis based on photos on as-cut bricks of multicrystalline Silicon (mc-Si), which we call "GFVis" (Growth Front Visualization). Subsequently, we show how a casting process for mc-Si can help to optimize a crystallization recipe for a cast-mono process with regard to phase front engineering. The mono-crystalline part over the whole ingot height shall be maximized by restricting parasitic grains to the outermost ingot margins whereas the phase front in the inner parts should rather be planar to keep stress low.

Keywords: Crystallization, growth front, image processing, directional solidification

1 INTRODUCTION

The silicon photovoltaics market has been largely dominated by Czochralzski Silicon (Cz-Si) for high efficiencies and multicrystalline silicon (mc-Silicon) for lower costs [2]. Recent advancement in crystallization techniques in cast-mono crystalline silicon attempt to make the best of both worlds in terms of cost and efficiency [3, 4]. Limiting the sub grains, the efficiency of the cast-mono material can be improved, since the dislocation development in silicon ingots can be traced to the absorption of stress and formation of grain boundaries in sub grains [5]. The planarity of the growth front during solidification of silicon crystals plays a vital role in controlling the grain boundary development [6].

The phase boundary during crystallization defined as the the interface between the silicon melt and the solidified crystal can be determined by numerical simulations from thermal gradient distribution as in [7–9]. In [10], the axial temperature distribution is measured in real time from the crucible wall and a 2D model is fit to estimate the phase boundary. These methods would require cost intensive temperature gradient monitoring during silicon crystal growth.

In-situ methods like X-ray topography are used to detect melt interface as in [11, 12]. Using travelling magnetic fields, the interface between the molten and solid silicon is identified [13]. In [14] lateral photo voltage scanning (LPS) method is used to detect the phase boundary from striations patterns on the crystal. However, these methods would require slicing of the ingot and additional polishing of the surfaces.

Recently in [15] a phase boundary detection method based on infrared images is proposed. The inclusions present in the ingot are detected and a polynomial plane is fit to estimate the phase in 3D. However, this method relies on the presence of inclusions in the material.

We introduce a simple yet novel approach to detect the phase-boundary automatically from optical images of sawn brick sides of multicrystalline ingots. We compare the phase boundary using our method to existing methods. The simplicity of the measurement approach offers compelling advantages:

- Non-destructive measurement of squared bricks without any additional brick preparation.
- Fast feedback is possible directly after squaring the ingot and before cropping and wafering
- Low-cost material requirements for the measurements (basically camera and an illumination source)
-

Grain-boundaries visible on the brick surface are the basis for *GFVis* to work. The orientation of the grain growth usually depends on the direction of the phase boundary. By estimating the direction of grain growth, it is possible to detect the phase boundary during directional solidification of silicon ingots.

The dependency on grain boundaries makes the method eligible for mc-Si material only. In cast-mono production, it is still advisable for crystal growers to realize the ramp-up of the crystallization process on mc-Si and later use the predeveloped crystallization process for cast-mono production. The phase-boundary information allows immediate feedback on the homogeneity of the growth process and speeds up the optimization of the furnace and the thermal process. This benefits in saving expensive monocrystalline seeds until the phase boundary has the desired shape.

The suggested approach allows a systematic and efficient process development towards reducing parasitic grain growth. Thus, the yield of pure monocrystalline wafers in cast-mono ingot growth with higher efficiencies can be increased further helps making the cast-mono growth technology as cost-competitive as mc-Silicon.

2 APPROACH

2.1 Physical assumption and concept

Under most industrial growth conditions, grain boundaries develop in growth direction roughly

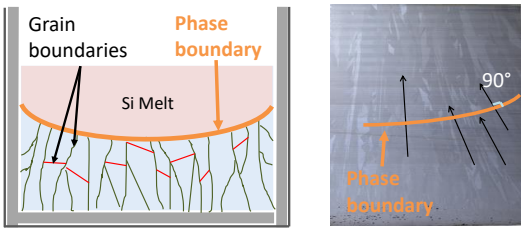

Figure 1: (Left) Schemata of the crystallization process and (right) exemplary optical image showing the assumed relationship of phase boundary (orange) and grain growth. Red lines indicate twin grain boundaries.

perpendicular to the phase front except for twin boundaries. This generalizing assumption is microscopically valid when the crystal surface is atomically rough on both sides of the grain boundary [16] during growth. We make use of this relationship and consider the angle of the grain boundaries in growth direction as indicator for the phase boundary. Figure 1 visualizes our approach which we refer to in the following as "Growth Front Visualization (GFVis)". Except for twin boundaries, we assume a perpendicular development of the grain boundaries to the phase front.

2.2 Measurement setup

In order to detect a sufficient amount of grain boundaries, sharp and high-resolution images of the brick sides are taken under different illumination angles. The images are captured directly after squaring before polishing the bricks to avoid strong reflectance. The measurement setup consists of a simple and cost effective setting: a camera on a tripod with remote release, a spotlight and a table for the brick samples. A sequence of photos is taken on the brick side, while the brick is illuminated from different directions a shown in Figure 2. The current prototype version of the measurement setting is built up manually so far and can be automated.

2.3 Algorithm

According to the mentioned assumption, the phase boundary is detected from the normal to the grain boundary angles. Therefore, the grain boundaries are detected in the photos and their growth angle is determined. A polynomial fit is applied to fit a curve for this purpose. The polynomial functions serve for visualization but they also allow for a quantitative comparison like local (height) extrema or curvature changes and extrema.

Thus, the algorithm consists of three major steps to detect the phase boundary from the measured optical images. The intermediate results for each step are presented in **Error! Reference source not found.**.

1. The input consists of optical images from the sides of unpolished as-cut bricks. These images are named according to ingot and brick position. Unsuitable images are removed manually to avoid detection errors. A semi-automatic alignment is applied, followed by an automatic pre-processing to remove noise. Each brick is identified in the images, segmented and rectified which results in a metric representation of the data (**Error! Reference source not found.**a).
2. Using image-processing techniques, grain boundaries are extracted from these images. By using controllable filters, the orientations of the grain boundaries are estimated from the orientation of the filter with the highest filter response (**Error! Reference source not found.**b). The 2D-normals of the grain boundaries are perpendicular to the filter orientation (**Error! Reference source not found.**c).
3. The normals computed serve as input for a polynomial fit in 2D. Twin grain boundaries should not be considered in the final mathematical model. Therefore, we exclude grain boundaries with very shallow growth orientations from the dataset used for fitting the polynomial. Furthermore, we apply a random sample consensus (RANSAC) algorithm [17], which evaluates the most plausible data during the fit. The resulting polynomial function yields the continuous information on the phase boundary (**Error! Reference source not found.** d).

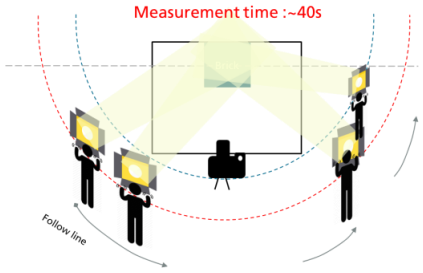

Figure 2: A simple measurement setup with distinct illumination angles

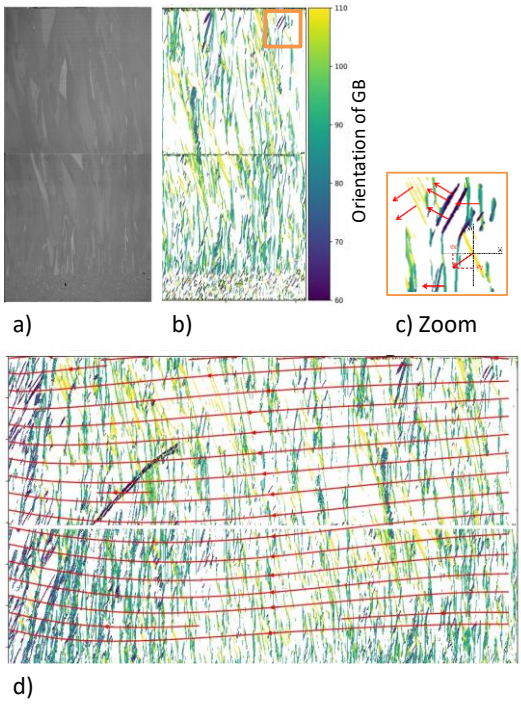

Figure 3: Intermediate results of our algorithm: a) optical image of a brick after segmentation and rectification, b) extracted grain boundaries and grain orientations by means of controllable filters, c) zoom image with orientation vectors and d) reconstructed phase front of three bricks by fitting a polynomial function to the gradients.

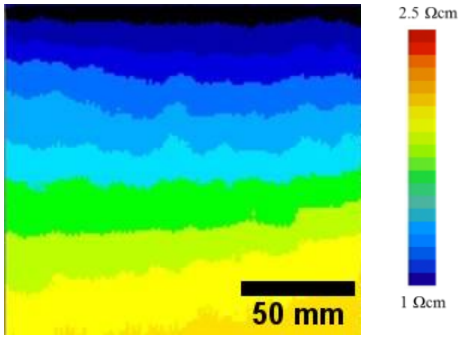

a) Resistivity mapping

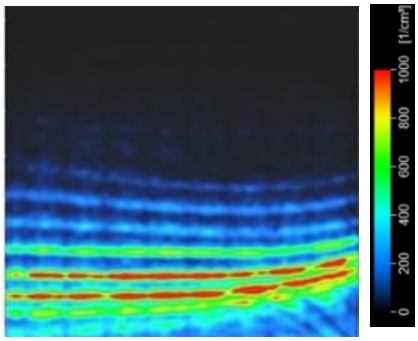

b) Inclusions from infrared-inclusion-imaging

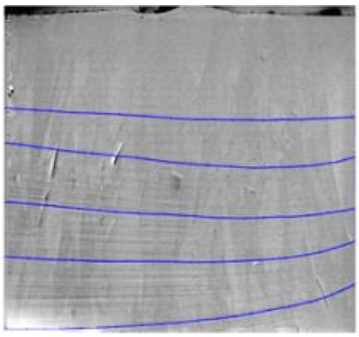

c) Lateral photo-voltage scanning

d) Photo-reconstruction (our GFVis approach)

Figure 4: Comparison of different methods for phase boundary determination on the same side of a brick from the ingot margin. a) Resistivity mapping (false colors). b) Infrared transmission measurements (color: number of particles per cm³, mostly SiC and Si_3N_4). c) Lateral Photovoltage scan, overlay of blue lines marking the lines along the doping level fluctuations d) Results obtained with GFVis

2.4 Validation of the method

For exemplary bricks, the results based on our method are compared to other phase boundary determination methods. These include:

- Lateral Photovoltage Scanning (LPS) [18], which is an established (but destructive) method for phase boundary determination
- Resistivity mapping, which roughly shows the isolines of resistivity indicating the phase boundary situation for various brick heights
- Inclusions (mainly SiC and Si_3N_4) from infrared transmission measurements – maxima of inclusions may occur at the growth front due to certain events like decreasing temperature gradients or convection slowing down

A quantitative comparison between LPS and *GFVis* is realized by identifying the doping level fluctuations in LPS via image processing for edge detection and orientation mapping. Similar to the *GFVis* approach, a dense vector field is calculated by fitting polynomials to the resulting vector field. Due to the extensive sample preparation and measurement procedure, only one brick measurement is available in that row.

2.5 Experimental setting:

We show comparative results on two industrial multicrystalline ingots (size G6) with different thermal processes.

- *Reference process:* The phase boundary is concave near the crucible due to larger temperature gradients
- *Engineered process:* The power is increased for the side heaters to flatten the boundary form near the crucible

Both ingots were grown under otherwise almost identical conditions.

3 METHOD VALIDATION

As already mentioned in section 2.4, ´the results obtained with our method are validated against other methods for phase front measurements, namely LPS, resistivity mapping, and infrared transmission measurements of inclusions in the brick. The obtained results are discussed in the following:

3.1 Visual judgment

The images in Figure 4 show different measurements on the same vertical brick side (the crucible wall being located on the right hand side in each image). It can be observed that the *GFVis* results shown in Figure 4 d) correspond well to the LPS results shown in Figure 4 c), and also to the inclusion levels, see Figure 4 b). The resistivity mapping (Figure 4 a)) gives a very rough image but a similar trend can also be observed there, in particular towards the ingot border on the right hand side of the images.

3.2 Quantitative comparison between LPS and *GFVis*

The difference between the LPS and *GFVis* results is quantified via a polynomial fit on the lines identified in LPS. In Figure 5 a) and b), the results of the fit are shown, in c), the distance between the polynomial functions in terms of angle distance is shown. Whereas in certain regions (black in the false color image) both

methods yield an almost identical orientation, the center of the shown region and the upper and left margins show higher deviations. Errors are discussed in Section 5.1.

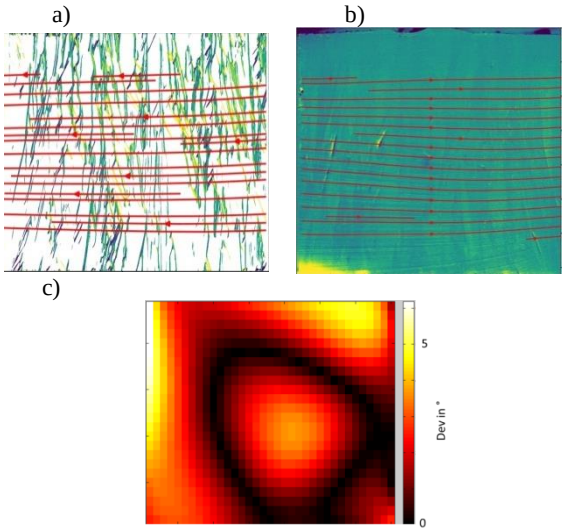

Figure 5: Results of quantitative comparison between the measurements. (Top) Fit based on results image of a) the optical images, b) the lateral photovoltage scanning and shown with red lines. c) Orientation difference between both methods using a polynomial fit in degrees.

4 PHASE BOUNDARY ENGINEERING

We evaluate the applicability of *GFVis* for two industry ingots of size G6: a reference ingot and an engineered one. The strong impact of the process variation is depicted in the results: It can be observed in **Error! Reference source not found.** b) that for the engineered process the phase boundary is convex (bent down) at the ingot margins, which is the desired case for restricting the parasitic grains. In contrast, in the original reference process (**Error! Reference source not found.** a), it is concave (bent up) at the same end.

5 DISCUSSION

5.1 Validation

Judgment by eye indicates that the methods yield comparable results, especially with the established LPS. The downsides of the other methods are the following;

- LPS requires a destructive preparation of the brick sides.
- Inclusions are not found in all heights or all ingots and the aim is to reduce them.
- Resistivity measurements only provide a rough insight into the phase boundary

Therefore, our non-destructive method is a valid and valuable tool for the visualization, analysis and assessment of the phase front.

The quantitative comparison shows deviations that are partly about 4-5°. These rather high values have two main reasons. One is that the polynomial fit is eventually not exact enough. Functions of higher order or splines could be evaluated instead. The other reason is that the evaluated image region for the *GFVis* method is considerably larger than that of the LPS method. For LPS, only one brick was available in one view, whereas the optical images are stitched for the brick sides before

a) Reference process

b) Engineered process

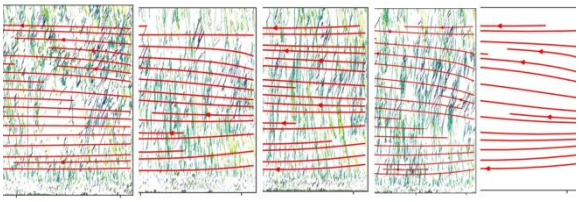

Figure 6: West side view on south ingot part, rows 1-5, GFVis results with phase front plot (red stream lines over identified grain boundaries) for a) reference process and b) engineered process.

the phase boundary is fitted. In Figure 5 a) one can observe that on the right hand side the actual lines display a higher curvature than the red polynomial level lines. Additionally, disturbing influences by twin structures are only considered indirectly within our approach. A targeted detection of twin grain boundaries can further avoid fitting errors.

LPS, on the other hand, does not display the same level of detail in all parts of the brick sides. As a result, we can assume that both methods are similar enough and that *GFVis* can be further optimized by following the discussed suggestions.

5.2 Phase boundary engineering

The results shown in **Error! Reference source not found.** prove that the heater setting is crucial for phase front engineering. *GFVis* serves as quantification for bending down the phase front through stronger lateral heating. Furthermore, the results support the idea that heater setting and the development angle of grain boundaries are connected in the expected way. *GFVis* is thus a suitable tool to monitor process improvements. A drawback of our method is that it is applicable only for material with enough grain boundaries, which prevents its direct application on cast-mono material. However, the process can be engineered on HP mc-Si and afterwards applied on a cast-mono setting. This approach could be advisable also for reasons of cost.

5.3 Method setup: state of automatization

While the algorithm can easily implemented on most platforms, up to now, most parts of the measurement are not fully automated yet but can be realized without much effort. This includes a setup with multiple illumination sources or a moving illumination source, and a fully automated alignment. On the other hand, the setting as described and applied in our case works well and is non-costly in purchase. For application in research or occasional use in industry, the stage of automatization can be judged as adequate.

6 CONCLUSION

We introduce a simple yet novel approach to reconstruct the phase-boundary from optical images of

brick sides. The method requires that most grain boundaries develop perpendicular to the crystallization front. The presented procedure attempts a non-destructive quality inspection of the crystallization process. We create promising results based on optical images of unpolished bricks by means of image processing algorithms.

We evaluated the method by comparing our results to alternative approaches, i.e., resistivity mapping, infrared-transmission imaging and lateral photo-voltage scanning. The results correlate qualitatively well with alternative methods. Compared to the alternative approaches, the method is less complex and expensive. A quantitative comparison of the optical reconstruction to lateral photo-voltage scanning shows deviations in angle of the reconstructed phase-fronts up to 5 degrees. These relatively large differences can be reduced by replacing the global polynomials chosen for the fit by splines and avoiding disturbances due to twin boundaries.

Overall, our method proves a valid and valuable tool for the visualization, analysis and assessment of the phase front and thus enables a systematic optimization of crystal growth processes with short feedback loop.

ACKNOWLEDGMENTS

This work was funded by the German Ministry for Economic Affairs and Energy (BMWi) within the frame of the project “Q-Crystal” (contract number 0324103A). Further, we thank Mr. Schöbel from Logomatic GmbH for the measurements.

7 REFERENCES

[1] K. Fujiwara and T. Tan, “Crystal Growth Behaviors of Silicon during Melt Growth Processes,” *International Journal of Photoenergy*, vol. 2012, p. 169829, 2012.

[2] ITRPV, “International Technology Roadmap for Photovoltaic,” 2020.

[3] M. Kivambe, B. Aissa, and N. Tabet, “Emerging Technologies in Crystal Growth of Photovoltaic Silicon: Progress and Challenges,” *Energy Procedia*, vol. 130, pp. 7–13, 2017.

[4] N. Stoddard, B. Wu, I. Witting, M. Wagener, G. Rozgonyi, and R. Clark, “Casting Single Crystal Silicon: Novel Defect Profiles from BP Solar’s Mono$^{2\,TM}$ Wafers,” *Solid State Phenomena*, vol. 131, pp. 1–8, 2008.

[5] B. Ryningen, G. Stokkan, M. Kivambe, T. Ervik, and O. Lohne, “Growth of dislocation clusters during directional solidification of multicrystalline silicon ingots,” *Acta Materialia*, vol. 59, no. 20, pp. 7703–7710, 2011.

[6] C. W. Lan, W. C. Lan, T. F. Lee, A. Yu, Y. M. Yang, W. C. Hsu, B. Hsu, and A. Yang, “Grain control in directional solidification of photovoltaic silicon,” *Journal of Crystal Growth*, vol. 360, pp. 68–75, 2012.

[7] K. Surovovs, M. Plāte, and J. Virbulis, “The Modelling of Phase Boundaries and Melt Flow in the Crucible-free Silicon Crystal Growth Using High-frequency Induction Heating,” in *Proceedings of the VIII International Scientific Colloquium "Modelling for Materials Processing"*, 2017.

[8] G. Ratnieks, A. Muižnieks, and A. Mühlbauer, “Modelling of phase boundaries for large industrial FZ silicon crystal growth with the needle-eye technique,” *Journal of Crystal Growth*, vol. 255, no. 3, pp. 227–240, 2003.

[9] Q. Lian, W. Liu, R. Li, W. Yan, C. Liu, Y. Zhang, L. Wang, and H. Chen, “Numerical Simulation of Multi-Crystalline Silicon Crystal Growth Using a Macro–Micro Coupled Method during the Directional Solidification Process,” *Applied Sciences*, vol. 7, no. 1, p. 21, 2017.

[10] J. Ding and L. Liu, “Real-time prediction of crystal/melt interface shape during Czochralski crystal growth,” *CrystEngComm*, vol. 20, 2018.

[11] K. Kakimoto, M. Eguchi, H. Watanabe, and T. Hibiya, “In-situ observation of solid-liquid interface shape by X-ray radiography during silicon single crystal growth,” *Journal of Crystal Growth*, vol. 91, no. 4, pp. 509–514, 1988.

[12] A. Tandjaoui, N. Mangelinck-Noël, G. Reinhart, J.-J. Furter, B. Billia, T. Lafford, J. Baruchel, and X. Guichard, “Real Time Observation of the Directional Solidification of Multicrystalline Silicon: X-ray Imaging Characterization,” *Energy Procedia*, vol. 27, pp. 82–87, 2012.

[13] N. Dropka and F. Kiessling, “Scale up of DS-silicon growth process under TMF,” in 2015.

[14] N. V. Abrosimov, A. Lüdge, H. Riemann, and W. Schröder, “Lateral photovoltage scanning (LPS) method for the visualization of the solid–liquid interface of Si1−xGex single crystals,” *Journal of Crystal Growth*, vol. 237-239, pp. 356–360, 2002.

[15] Y. Hayama, T. Matsumoto, T. Muramatsu, K. Kutsukake, H. Kudo, and N. Usami, “3D visualization and analysis of dislocation clusters in multicrystalline silicon ingot by approach of data science,” *Solar Energy Materials and Solar Cells*, vol. 189, pp. 239–244, 2019.

[16] T. Duffar and A. Nadri, “The grain–grain–liquid triple phase line during solidification of multi-crystalline silicon,” *Comptes Rendus Physique*, vol. 14, no. 2-3, pp. 185–191, 2013.

[17] M. A. Fischler and R. C. Bolles, “Random Sample Consensus: A Paradigm for Model Fitting with Applications to Image Analysis and Automated Cartography,” *Commun. ACM*, vol. 24, no. 6, pp. 381–395, 1981.

[18] A. Lüdge and H. Riemann, “Doping inhomogeneities in silicon crystals detected by the lateral photovoltage scanning (LPS) method,” in *CONFERENCE SERIES-INSTITUTE OF PHYSICS*, 1998, pp. 145–148.